Role of Vibronic Couplings and Energy Gap in the Internal Conversion Process of a Molecule

Wataru Ota,[†,‡] Motoyuki Uejima,[¶] and Tohru Sato[*,†,‡]

†*Fukui Institute for Fundamental Chemistry, Kyoto University, Takano Nishibiraki-cho 34-4, Sakyo-ku, Kyoto 606-8103, Japan*

‡*Department of Molecular Engineering, Graduate School of Engineering, Kyoto University, Nishikyo-ku, Kyoto 615-8510, Japan*

¶*MOLFEX, Inc., Takano Nishibiraki-cho 34-4, Sakyo-ku, Kyoto 606-8103, Japan*

E-mail: tsato@scl.kyoto-u.ac.jp

Abstract

In this study, an analytical expression for the rate constant of the internal conversion (IC) in a molecule was derived based on the crude adiabatic representation. All vibrational modes were considered to be on equal footing in the rate constant expression. Based on this expression, we investigated the role of vibronic couplings and electronic energy gap in IC processes, using 9-fluorenone as an illustrative example. Vibrational modes with strong off-diagonal vibronic coupling constants (VCCs) give rise to non-radiative transitions. Contrastingly, vibrational modes with strong diagonal VCCs constitute the final vibronic states that accept the excess energy between the initial and final electronic states. Therefore, vibrational modes are classified into promoting and accepting modes based on their roles. We identified important promoting modes responsible for the one-phonon emission/absorption and accepting modes that contribute greatly to the final state. A Franck-Condon (FC) envelope describes the final density of vibronic states and explains the dependence of the rate constant on

the energy gap. VCC can be visualized as a spatial distribution of its density form, i.e., vibronic coupling density (VCD), obtained from the electronic wave functions and vibrational modes. Using the concept of VCD, the IC process can be understood and controlled in terms of the electronic states and vibrational modes. This approach provides new chemical insights into IC processes. It has the advantage that the VCD concept facilitates the design of functional molecules with IC processes controlled.

INTRODUCTION

A transition between electronic states is classified into radiative or nonradiative, depending on whether a photon or phonon induces the transition.[1] The nonradiative transition between electronic states with the same spin multiplicity is called internal conversion (IC), whereas that with a different spin multiplicity is called intersystem crossing (ISC). The theory of IC has been studied for decades.[2–12] The rate constant of the IC depends on both the electronic energy gap and vibronic couplings. It is well known that the rate constant has an exponential dependence on the electronic transition energy in the weak coupling limit, that is, the so-called energy gap law.[9,10] Contrastingly, the relationship between the rate constant and vibronic couplings remains unclear. This is attributed to the difficulty in computing the rate constant by incorporating all vibrational modes with different vibronic coupling constants (VCCs). Shuai *et al.* derived an expression for the IC rate constant in a time-correlation function formalism, where the density of vibronic states weighted by a matrix element of multi-mode vibrational states is evaluated using an analytical path integral solution of a multi-dimensional harmonic oscillator.[13–15] This path integral approach has the advantage of efficiently calculating the rate constant by considering all vibrational modes, and has been widely employed by several authors.[16–21] Notably, the analytical solution using the vibrational correlation function has long been well-known.[4,9,12]

Formulations of the IC rate constant are commonly based on the Born–Oppenheimer (BO) representation.[2,8,14] The BO and crude adiabatic (CA) representations are well-known

to treat nuclear motions in a molecule.[22,23] In the BO representation, the vibronic wave function is expanded by electronic wave functions depending on nuclear coordinates called the BO basis. In contrast, the vibronic wave function in the CA representation is expanded by electronic wave functions fixed at a reference nuclear configuration called the CA basis. Sato *et al.* have investigated vibronic couplings using the CA representation through vibronic coupling density (VCD), with which the local picture of a vibronic coupling is elucidated from the electronic and vibrational structures of a molecule.[24–26] VCD has been utilized to determine the origin of vibronic couplings for various fluorescent molecules,[27–32] and has been applied to the design of novel compounds without requiring computational screening.[33–35] In other words, the formulation using the CA representation can provide chemical insights into vibronic couplings and enable rational molecular design.

Thus, we can expect detailed insights into the IC process from an expression of the IC rate based on the CA representation, where the VCCs and the energy gap are incorporated. In this study, we derived the IC rate expression based on the CA representation, and investigated the role of the energy gap and vibronic couplings in the IC processes through the analytical expression that included all vibrational modes on an equal footing. We focused on the vibrational modes that contribute to the IC processes. 9-Fluorenone, in which the IC and ISC rate constants have been previously observed in experiments,[36–38] was used as an example.

THEORY

Rate Constants of Internal Conversion and Fluorescence

We considered a molecule consisting of M nuclei and N electrons. A set of electronic coordinates is denoted by $\mathbf{r} = (\mathbf{r}_1, \cdots, \mathbf{r}_i, \cdots, \mathbf{r}_N)$ where $\mathbf{r}_i = (x_i, y_i, z_i)$ in the Cartesian coordinates, and a set of mass-weighted normal coordinates is denoted by $\mathbf{Q} = (Q_1, \cdots, Q_\alpha, \cdots, Q_{3M-5 \text{ or } 3M-6})$. Since we considered the stable structure of the initial electronic state as a reference nuclear configuration, molecular deformation from the stable structure is described by the normal

coordinates. To express a vibronic wave function, we employed the CA basis, $\{\Psi_m(\mathbf{r},\mathbf{0})\}$, where the electronic wave function $\Psi_m(\mathbf{r},\mathbf{0})$ is fixed at the reference nuclear configuration, that is, $\mathbf{Q}=\mathbf{0}$. This differs from the BO basis, $\{\Psi_m(\mathbf{r},\mathbf{Q})\}$, where the electronic wave function $\Psi_m(\mathbf{r},\mathbf{Q})$ depends on the nuclear coordinates. A matrix representation of the vibronic Hamiltonian $\mathcal{H}(\mathbf{r},\mathbf{Q})$ employing the CA basis is given by (for details, see Sec. S1.1 in the Supporting Information)[24,39]

$$\begin{aligned}&\langle\Psi_n(\mathbf{r},\mathbf{0})|\mathcal{H}(\mathbf{r},\mathbf{Q})|\Psi_m(\mathbf{r},\mathbf{0})\rangle\\&=\left(E_m(\mathbf{0})+\sum_\alpha\left(-\frac{\hbar^2}{2}\frac{\partial^2}{\partial Q_\alpha^2}+V_{m,\alpha}Q_\alpha+\frac{\omega_\alpha^2}{2}Q_\alpha^2\right)\right)\delta_{nm}+\sum_\alpha V_{nm,\alpha}Q_\alpha(1-\delta_{nm}).\end{aligned}\tag{1}$$

Here, in the diagonal element, (i) up to the quadratic orders are considered, and (ii) the Duschinsky rotation effect[40] is neglected, which is the Hamiltonian of a displaced harmonic oscillator. In the off-diagonal element, up to the linear order is considered. In the above equation, $\hbar$ is the Dirac constant, $E_m(\mathbf{0})$ is the electronic energy at $\mathbf{Q}=\mathbf{0}$, and ω_α is the angular frequency of vibrational mode α. Additionally, $V_{nm,\alpha}$ is a linear VCC defined by

$$V_{nm,\alpha}=\langle\Psi_n(\mathbf{r},\mathbf{0})|\mathcal{V}_\alpha|\Psi_m(\mathbf{r},\mathbf{0})\rangle\,,\tag{2}$$

where $\mathcal{V}_\alpha$ denotes the electronic part of the linear vibronic coupling operator (Eq. (S9)). Particularly, $V_{m,\alpha}:=V_{mm,\alpha}$ with $n=m$ is called the diagonal VCC, and $V_{nm,\alpha}$ with $n\neq m$ is called the off-diagonal VCC. The direction of the vibrational mode is considered such that the VCC is negative, that is, $V_{nm,\alpha}=-|V_{nm,\alpha}|$. The diagonal vibronic couplings cause vibrational relaxation, and the off-diagonal vibronic couplings cause transitions between the different electronic states. The off-diagonal matrix element in the CA basis is the vibronic coupling whereas that in the BO basis is the derivative coupling.[22,23] This difference between the CA and BO bases leads to different expressions for the IC rate constant.

We considered IC from the initial electronic state m to the final state n within the CA approximation. Within this approximation, a vibronic wave function, $\Phi_{m\nu}(\mathbf{r},\mathbf{Q})$, is

expressed as the product of the electronic and vibrational wave functions, $\chi_{m\nu}(\mathbf{Q})$, with $\nu = (\nu_1, \cdots, \nu_\alpha, \cdots, \nu_{3M-5 \text{ or } 3M-6})$ being a set of vibrational quantum numbers:[22,23]

$$\Phi_{m\nu}(\mathbf{r}, \mathbf{Q}) = \chi_{m\nu}(\mathbf{Q})\Psi_m(\mathbf{r}, \mathbf{0}). \tag{3}$$

Therefore, we considered the vibronic transitions from $|\Phi_{m\nu}\rangle = |\chi_{m\nu}\rangle |\Psi_m\rangle$ to $|\Phi_{n\nu'}\rangle = |\bar{\chi}_{n\nu'}\rangle |\Psi_n\rangle$, treating the off-diagonal matrix element of the vibronic Hamiltonian as a perturbation. The reference nuclear configuration $\mathbf{Q} = 0$ is taken at the equilibrium geometry of the initial electronic state m, indicating $V_{m,\alpha} = 0$ for all vibrational modes. It should be emphasized that within the CA approximation, the final electronic state does not need to be geometrically optimized because the displacement from the minimum of the initial electronic state to that of the final state along vibrational mode α is given by $V_{n,\alpha}/\omega_\alpha^2$, and the reorganization energy of the final electronic state is given by $V_{n,\alpha}^2/2\omega_\alpha^2$ (Sec. S1.2).

According to Fermi's golden rule, the IC rate constant from the initial electronic state m to the final state n is given by[27]

$$k_{n\leftarrow m}^{\mathrm{IC}} = \frac{2\pi}{\hbar} \sum_{\nu,\nu'} P_{m\nu}(T) |(\mathbf{H}')_{nm}|^2 \delta(E_{n\nu'} - E_{m\nu}), \tag{4}$$

where the perturbation is the off-diagonal matrix element of the vibronic Hamiltonian, that is,

$$(\mathbf{H}')_{nm} = \sum_\alpha V_{nm,\alpha} \langle \bar{\chi}_{n\nu'} | Q_\alpha | \chi_{m\nu} \rangle . \tag{5}$$

$P_{m\nu}(T) = \prod_\alpha P_{m\nu_\alpha}(T)$ is a distribution of the initial vibrational states, which is represented by Boltzmann's distribution at temperature T in this study, assuming that the initial state is in the thermal equilibrium. $E_{m\nu}$ and $E_{n\nu'}$ are the vibronic energies of the initial and final vibronic states, respectively (Eqs. (S17) and (S20)). Thus, the rate constant can be written

as:[27]

$$k^{\mathrm{IC}}_{n\leftarrow m} = \sum_{\alpha,\beta} k^{\mathrm{IC}}_{n\leftarrow m,\alpha\beta}, \tag{6}$$

$$k^{\mathrm{IC}}_{n\leftarrow m,\alpha\beta} = \frac{2\pi}{\hbar} V_{nm,\alpha} V_{mn,\beta} \Theta_{\alpha\beta}, \tag{7}$$

where $\Theta_{\alpha\beta}$ denotes the final density of vibronic states weighted by the vibrational matrix element,

$$\Theta_{\alpha\beta} = \sum_{\nu,\nu'} P_{m\nu}(T) \left\langle \bar{\chi}_{n\nu'} | Q_\alpha | \chi_{m\nu} \right\rangle \left\langle \chi_{m\nu} | Q_\beta | \bar{\chi}_{n\nu'} \right\rangle \delta(E_{n\nu'} - E_{m\nu}). \tag{8}$$

The vibrational matrix element is given by[27]

$$\left\langle \bar{\chi}_{n\nu'} | Q_\alpha | \chi_{m\nu} \right\rangle = \left\langle \bar{\nu}'_\alpha | Q_\alpha | \nu_\alpha \right\rangle \prod_{\beta\neq\alpha} \left\langle \bar{\nu}'_\beta | \nu_\beta \right\rangle, \tag{9}$$

$$\left\langle \bar{\nu}'_\alpha | Q_\alpha | \nu_\alpha \right\rangle = \sqrt{\frac{\hbar}{2\omega_\alpha}} \left(\sqrt{\nu_\alpha + 1} \left\langle \bar{\nu}'_\alpha | \nu_\alpha + 1 \right\rangle + \sqrt{\nu_\alpha} \left\langle \bar{\nu}'_\alpha | \nu_\alpha - 1 \right\rangle \right), \tag{10}$$

where $|\nu_\alpha\rangle$ and $|\bar{\nu}_\alpha\rangle$ are the initial and final single-mode vibrational states, respectively. The FC overlap integral between the initial and final vibrational states is given by[41,42]

$$\left\langle \bar{\nu}'_\alpha | \nu_\alpha \right\rangle = \sqrt{\frac{\nu_\alpha ! \nu'_\alpha !}{2^{\nu_\alpha + \nu'_\alpha}}} e^{-\frac{g^2_{n,\alpha}}{4}} \sum_{l=0}^{\min[\nu_\alpha \nu'_\alpha]} (-1)^{\nu_\alpha - l} 2^l \frac{g_{n,\alpha}^{\nu_\alpha + \nu'_\alpha - 2l}}{l!(\nu_\alpha - l)!(\nu'_\alpha - l)!}, \tag{11}$$

which depends on the dimensionless diagonal VCC, $g_{n,\alpha} := V_{n,\alpha}/\sqrt{\hbar\omega^3_\alpha}$.[43] Note that $\langle \bar{\nu}'_\alpha | \nu_\alpha \rangle = \delta_{\nu'_\alpha,\nu_\alpha}$ when $g_{n,\alpha} = 0$, or when the final electronic state is not displaced with respect to the initial state, because it is orthonormalized.

Next, we discuss the selection rule for the integrals and factors that appear in the IC rate expression. The selection rule in $k^{\mathrm{IC}}_{n\leftarrow m,\alpha\beta}$ is divided into $V_{nm,\alpha}$ and $\Theta_{\alpha\beta}$ (Eq. (7)). The off-diagonal VCC, $V_{nm,\alpha}$, is non-vanishing when the irreducible representation of vibrational mode α, Γ_α, is contained in the product of the irreducible representations of the initial and final electronic states, $\Gamma_n \times \Gamma_m$, that is, $\Gamma_\alpha \in \Gamma_n \times \Gamma_m$.[43] The vibrational mode with non-zero

$V_{nm,\alpha}$ responsible for a vibronic transition is called a promoting mode.[2,7] The diagonal VCC, $V_{n,\alpha}$, is non-vanishing when $\Gamma_\alpha \in [\Gamma_n^2]$.[43] The vibrational mode with non-zero $V_{n,\alpha}$ is called an accepting modes because this mode, along which a potential energy surface is displaced, mainly accepts excess electronic energy.[2,7] The density of states weighted by the vibrational matrix element, $\Theta_{\alpha\beta}$, is non-vanishing when $\alpha = \beta$ or $\alpha \neq \beta$ with $\Gamma_\alpha = \Gamma_\beta \in [\Gamma_n^2]$ (see Sec. S1.3). As a result, $k^{\mathrm{IC}}_{n\leftarrow m,\alpha\beta}$ is non-vanishing when $\alpha = \beta$ with $\Gamma_\alpha \in \Gamma_n \times \Gamma_m$ or $\alpha \neq \beta$ with $\Gamma_\alpha = \Gamma_\beta \in \Gamma_n \times \Gamma_m$ and $\Gamma_\alpha = \Gamma_\beta \in [\Gamma_n^2]$. The second condition is satisfied when a vibrational mode is both the promoting and accepting mode, which holds, for example, in the C_1 point group.

Suppose that vibrational mode α is a promoting mode but not an accepting mode, namely $V_{nm,\alpha} \neq 0$ and $V_{n,\alpha} = 0$. This assumption is valid for the IC from S_1 to S_0 in 9-fluorenone, as shown in the following section (the treatment for a general case is presented in Sec. S1.3.). In this case, since the initial and final vibrational states of promoting mode α are orthogonalized, $\Theta_\alpha := \Theta_{\alpha\alpha}$ can be transformed into (see Eqs. (8)–(10)),

$$\Theta_\alpha = \sum_{\nu_\alpha} P_{m\nu_\alpha}(T) \left[\left(\frac{(\nu_\alpha + 1)\hbar}{2\omega_\alpha} \right) F^{(\alpha)}(+\hbar\omega_\alpha) + \left(\frac{\nu_\alpha \hbar}{2\omega_\alpha} \right) F^{(\alpha)}(-\hbar\omega_\alpha) \right], \tag{12}$$

$$F^{(\alpha)}(E) = \sum_{\nu \not\ni \nu_\alpha} \sum_{\nu' \not\ni \nu'_\alpha} \prod_{\beta\neq\alpha} P_{m\nu_\beta}(T) |\left\langle \bar{\nu}'_\beta | \nu_\beta \right\rangle|^2 \delta \left(E_n - E_m + \sum_{\beta\neq\alpha} \hbar\omega_\beta(\nu'_\beta - \nu_\beta) + E \right). \tag{13}$$

Here, $F^{(\alpha)}(E)$ is the FC envelope with vibrational mode (promoting mode) α dropped. E_m and E_n are the energy minima of the potential energy surfaces for the initial and final electronic states, respectively (Eqs. (S21) and (S22)); therefore, $E_m - E_n$ represents the electronic energy gap. The energy in $F^{(\alpha)}(E)$ is the energy difference between the initial and final vibronic energies that excludes the vibrational energy of mode α. The first term in Eq. (12) indicates that the IC occurs at $E = +\hbar\omega_\alpha$ through the one-phonon emission of promoting mode α, whereas the second term with $E = -\hbar\omega_\alpha$ represents the one-phonon absorption. Particularly, phonon emissions with $\nu_\alpha = 0$ and $\nu_\alpha \neq 0$ correspond to spontaneous and stimulated emissions, respectively. Phonon absorption occurs when $\nu_\alpha \neq 0$. The final density of

vibronic states described by the FC envelope, which depends on the energy gap, diagonal VCCs, and frequencies of the accepting modes, receives excess electronic energy after phonon emission and absorption.

The present expression for the IC rate can be regarded as a phonon analog of the radiative transition (see Fig. 1). The rate constant from the initial vibronic state $m\nu$ to the final state $n\nu'$ by emitting a phonon of promoting mode α with energy $\hbar\omega_\alpha$ is expressed as (see Eqs. (7), (12), and (13))

$$k^{\text{phonon}}_{n\nu'\leftarrow m\nu,\alpha} = \frac{2\pi}{\hbar}|V_{nm,\alpha}|^2\frac{(\nu_\alpha+1)\hbar}{2\omega_\alpha}\prod_{\beta\neq\alpha}|\,\langle\bar{\nu}'_\beta|\nu_\beta\rangle\,|^2\delta\left(E_n-E_m+\sum_{\beta\neq\alpha}\hbar\omega_\beta(\nu'_\beta-\nu_\beta)+\hbar\omega_\alpha\right). \tag{14}$$

The rate constant from the initial vibronic state $m\nu$ to the final state $n\nu'$ by emitting a photon with energy $\hbar\omega_{\mathbf{k}}$, where $\omega_{\mathbf{k}}$ is the photon frequency with wavevector $\mathbf{k}$ and polarization λ, is given by[44,45]

$$k^{\text{photon}}_{n\nu'\leftarrow m\nu,\mathbf{k}\lambda} = \frac{2\pi}{\hbar}|\mathbf{e}_{\mathbf{k}\lambda}\cdot\boldsymbol{\mu}_{nm}|^2\frac{(\nu_{\mathbf{k}\lambda}+1)2\pi\hbar\omega_{\mathbf{k}}}{V}\prod_{\alpha}|\,\langle\bar{\nu}'_\alpha|\nu_\alpha\rangle\,|^2\delta\left(E_{n\nu'}-E_{m\nu}+\hbar\omega_{\mathbf{k}}\right). \tag{15}$$

Here, $\mathbf{e}_{\mathbf{k}\lambda}$ with $\lambda=1,2$ is the polarization vector, $\boldsymbol{\mu}_{nm}$ is the transition dipole moment between the electronic states m and n, $\nu_{\mathbf{k}\lambda}$ is the photon quantum number, and V is the volume. The matrix element of the perturbation between the electronic states is the off-diagonal VCC and transition dipole moment for the phonon and photon emissions, respectively. Note that, for photon emission, all vibrational modes appear in the expression of the final density of vibronic states.

The rate constant of fluorescence, or spontaneous photon emission, from the initial electronic state m to the final state n is given by[27]

$$k^{\text{f}}_{n\leftarrow m} = \int_0^\infty d\omega\ \frac{4\omega^3}{3c^3}|\boldsymbol{\mu}_{nm}|^2F^{(0)}(+\hbar\omega), \tag{16}$$

$$F^{(0)}(E) = \sum_{\nu,\nu'}P_{m\nu}(T)|\,\langle\bar{\chi}_{n\nu'}|\chi_{m\nu}\rangle\,|^2\delta(E_{n\nu'}-E_{m\nu}+E), \tag{17}$$

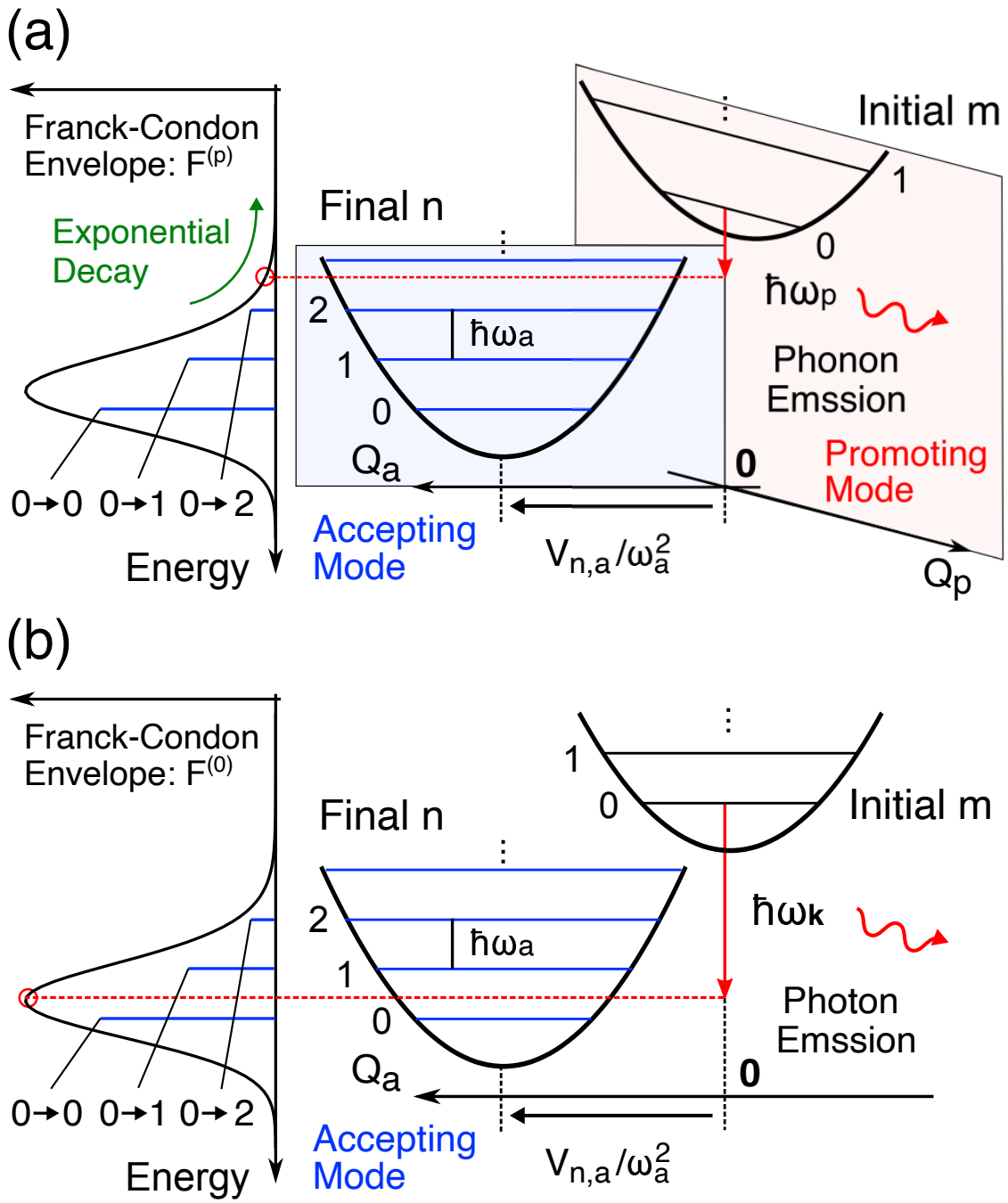

Figure 1: (a) Schematic diagram of a one-phonon emission process, where the phonon of a promoting mode is emitted while the excess electronic energy is mainly received by accepting modes. A reference nuclear configuration, $\mathbf{Q} = \mathbf{0}$, is set at the equilibrium geometry of the initial electronic state m. Displacement from the minimum of the initial electronic state to that of the final state along accepting mode a is given by $V_{n,a}/\omega_a^2$. (b) Schematic diagram of a one-photon emission process.

where c is the speed of a photon, and $F^{(0)}(E)$ is the FC envelope that includes all vibrational modes. Fluorescence occurs when $E = +\hbar\omega$, where ω is the continuous photon frequency. The integrand of Eq. (16) represents the fluorescence spectrum.

The FC envelope, Eq. (17), in the time-correlation function formalism is written as:[3,46]

$$F^{(0)}(E) = \frac{1}{2\pi}\int_{-\infty}^{\infty} d\tau\ \rho^{(0)}(\tau)e^{i(E_n - E_m + E)\tau}, \tag{18}$$

where τ is the time divided by $\hbar$, and $\rho^{(0)}(\tau)$ is the correlation function of the vibrational states. $F^{(0)}(E)$ in the time representation can be evaluated with a reasonable computational cost using the analytical expression of $\rho^{(0)}(\tau)$.[4,9,12,14] For displaced harmonic oscillators, $\rho^{(0)}(\tau)$ is given by[4,9]

$$\rho^{(0)}(\tau) = \prod_{\alpha} \rho_\alpha(\tau), \tag{19}$$

$$\rho_\alpha(\tau) = \exp\left(-\frac{g_{n,\alpha}^2}{2}(2n_\alpha + 1) + \frac{g_{n,\alpha}^2}{2}(n_\alpha + 1)e^{i\hbar\omega_\alpha\tau} + \frac{g_{n,\alpha}^2}{2}n_\alpha e^{-i\hbar\omega_\alpha\tau}\right), \tag{20}$$

where $n_\alpha = (e^{\hbar\omega_\alpha/kT} - 1)^{-1}$, where k is the Boltzmann constant, is the number of excited vibrations of mode α in thermal equilibrium. In the limit of $T \to 0$ K, since $n_\alpha \to 0$, $\rho_\alpha(\tau) = \exp(-g_{n,\alpha}^2/2 + g_{n,\alpha}^2 e^{i\hbar\omega_\alpha\tau}/2)$. The FC envelope with promoting mode α dropped, Eq. (13), is given in the time representation by

$$F^{(\alpha)}(E) = \frac{1}{2\pi}\int_{-\infty}^{\infty} d\tau\ \rho^{(\alpha)}(\tau)e^{i(E_n - E_m + E)\tau}, \tag{21}$$

$$\rho^{(\alpha)}(\tau) = \prod_{\beta\neq\alpha} \rho_\beta(\tau), \tag{22}$$

where $\rho^{(\alpha)}(\tau)$ is the correlation function of the vibrational states excluding promoting mode α.

In an actual situation, the density of the final vibronic states is continuous and broadened by the neglected interactions, including rovibronic states and interactions with a surrounding

environment with infinite degrees of freedom, such as other molecules or solvents. This broadening is expressed using a Gaussian function incorporating the linewidth, σ, in the Fourier transformed expression of $\rho^{(0/\alpha)}(\tau)e^{-\sigma^2\tau^2/2}$ instead of $\rho^{(0/\alpha)}(\tau)$ in Eqs. (18) and (21).

Vibronic Coupling Density

The origin of the VCC is investigated based on its density form, or the VCD. The VCD is given by an integrand of the VCC (for details, see Sec. S1.4);[24–26]

$$V_{nm,\alpha} = \int d\boldsymbol{x}\ \eta_{mn,\alpha}(\boldsymbol{x}), \tag{23}$$

where $\boldsymbol{x} = (x, y, z)$ is a three-dimensional Cartesian coordinate and

$$\eta_{nm,\alpha}(\boldsymbol{x}) = \begin{cases} \Delta\rho_{nm}(\boldsymbol{x}) \times v_\alpha(\boldsymbol{x}) & (n = m) \\ \rho_{nm}(\boldsymbol{x}) \times v_\alpha(\boldsymbol{x}) & (n \neq m) \end{cases}. \tag{24}$$

$\eta_{n,\alpha}(\boldsymbol{x}) := \eta_{nn,\alpha}(\boldsymbol{x})$ is called the diagonal VCD and $\eta_{nm,\alpha}(\boldsymbol{x})$ with $n \neq m$ is called the off-diagonal VCD. $\Delta\rho_{nm}(\boldsymbol{x})$ and $\rho_{nm}(\boldsymbol{x})$ are the electron density difference and overlap density between the electronic states m and n, respectively, and $v_\alpha(\boldsymbol{x})$ is the potential derivative of vibrational mode α. The VCD elucidates the local picture of vibronic coupling by separating it into electronic and vibrational structures (Fig. S1).

METHOD OF CALCULATION

The ground and excited electronic structures of 9-fluorenone were calculated at the B3LYP/6-31G(d,p) and TD-B3LYP/6-31G(d,p) levels of theory, respectively. The solvent effect of toluene was included through the polarizable continuum model (PCM).[47] The electronic and vibrational structures were computed using Gaussian 16 Revision C.01.[48]

The calculation methods for the VCC and VCD are described in Refs. 25 and 27. The

fluorescence spectrum and $k^{\mathrm{f}}_{n\leftarrow m}$ were calculated using Eqs. (16), and (18)–(20), whereas $k^{\mathrm{IC}}_{n\leftarrow m}$ was calculated using Eqs. (6), (7), (12), and (20)–(22). The FC factors were evaluated using Eq. (11). The VCC, VCD, fluorescence spectrum, $k^{\mathrm{f}}_{n\leftarrow m}$, and $k^{\mathrm{IC}}_{n\leftarrow m}$ were computed using in-house codes.

RESULTS AND DISCUSSION

Rate Constant of Internal Conversion

The geometrical structure of 9-fluorenone in the S_1 excited state was optimized with the C_{2v} symmetry. S_1 belonging to the B_2 irreducible representation mainly consists of the HOMO–LUMO transition, and has an oscillator strength of $f = 0.0121$ (Table S1 in the Supporting Information). The HOMO and LUMO are shown in Fig. S2.

Since the calculated value of the IC rate depends on the linewidth σ, we should determine σ based on a reliable physical basis or some experiment for the calculation of $k^{\mathrm{IC}}_{n\leftarrow m}$. We used the experimental fluorescence spectrum of 9-fluorenone[49] to determine σ. The fluorescence spectrum from S_1 to S_0 was calculated at $T = 300$ K (Fig. 2). The linewidth was determined so that the calculated spectrum reproduced the broadening of the experimental spectrum (Table S2). We determined the linewidth to be σ =400 cm^{-1}. This computational condition for the final density of vibronic states was employed to calculate the fluorescence and IC rate constants.

Table 1 summarizes the computed fluorescence and IC rate constants from S_1 to S_0 at $T = 300$ K. This result indicates that the final vibronic state was appropriately represented within the CA approximation. For example, the reorganization energies of S_0 from the S_1 to S_0 optimized structures are in good agreement between the CA (0.410 eV) and BO (0.397 eV) approximations. The value of the IC rate constant depends on the linewidth of the Gaussian function (Table S3); therefore, the linewidth should be determined carefully. We employed a linewidth of 400 cm^{-1} because it best reproduced the line shape of the

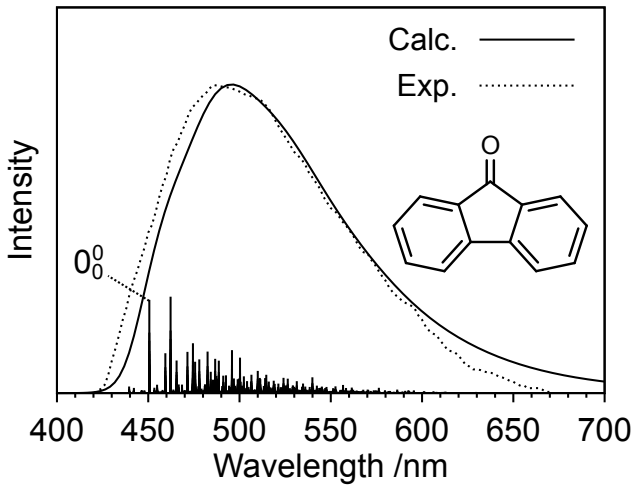

Figure 2: Calculated fluorescence spectrum from S_1 to S_0 of 9-fluorenone in toluene at $T = 300$ K, compared with the experimental spectrum.[49] The broadening of the density of the final vibronic states was expressed using the Gaussian function with a linewidth of 400 cm^{-1}. The vertical line shows the intensities of the FC factors, where 0_0^0 represents the FC factor of the 0–0 transition. The inset shows the structure of 9-fluorenone.

experimental fluorescence spectrum.

Table 1: Calculated fluorescence and IC rate constants from S_1 to S_0 of 9-fluorenone in toluene at $T = 300$ K. The density of the final vibronic states was expressed using the Gaussian function with a linewidth of 400 cm^{-1}.

	Calc.	Exp.[36]	Exp.[37]
$k^{\mathrm{f}}_{n\leftarrow m}$ /10^6 s^{-1}	3.0	2.7	3.2
$k^{\mathrm{IC}}_{n\leftarrow m}$ /10^7 s^{-1}	8.8	8.6	3.7

The contributing factors of the IC rate constant, $k^{\mathrm{IC}}_{n\leftarrow m}$, were examined from its vibrational decomposition, $k^{\mathrm{IC}}_{n\leftarrow m,\alpha\beta}$ (Eq. (6)). First, we discussed the selection rule of $k^{\mathrm{IC}}_{n\leftarrow m,\alpha\beta}$, in which that of the off-diagonal VCC, $V_{nm,\alpha}$, and the density of states weighted by the vibrational matrix element, $\Theta_{\alpha\beta}$ (Eq. (7)), were separated for discussion purposes. The reducible representation of the vibrational modes of 9-fluorenone with C_{2v} symmetry is decomposed as follows:

$$\Gamma_{\mathrm{vib}}(C_{2v}) = 21A_1 + 9A_2 + 10B_1 + 20B_2. \tag{25}$$

Since S_1 and S_0 belong to the B_2 and A_1 irreducible representations, respectively, the vibronic active mode for $V_{nm,\alpha}$ between S_1 and S_0 is B_2, that is, $\Gamma_\alpha = B_2$. Additionally, $\Theta_{\alpha\beta}$ is non-

vanishing when $\alpha = \beta$ with $\Gamma_\alpha = A_1, A_2, B_1$, and B_2 or $\alpha \neq \beta$ with $\Gamma_\alpha = \Gamma_\beta = A_1$. As a result, $k^{\rm IC}_{n\leftarrow m,\alpha\beta}$ is non-vanishing only when $\alpha = \beta$ with $\Gamma_\alpha = B_2$. Therefore, it is sufficient to consider the case $\alpha = \beta$. The vibronic active mode for the diagonal VCC, $V_{n,\alpha}$, of S_0 is the totally symmetric mode, A_1. Thus, the vibrational modes with $\Gamma_\alpha = B_2$ are the promoting modes and those with $\Gamma_\alpha = A_1$ are the accepting modes.

Figures 3 (a)–(c) show $k^{\rm IC}_{n\leftarrow m,\alpha} := k^{\rm IC}_{n\leftarrow m,\alpha\alpha}$ and its components, i.e., $|V_{nm,\alpha}|^2$ and Θ_α, plotted with respect to vibrational modes. The numbering of the vibrational modes is in ascending order of frequency. The primary promoting modes are modes 34 and 48, resulting in a large $k^{\rm IC}_{n\leftarrow m,\alpha}$. Therefore, we focused on the IC promoted by these modes below.

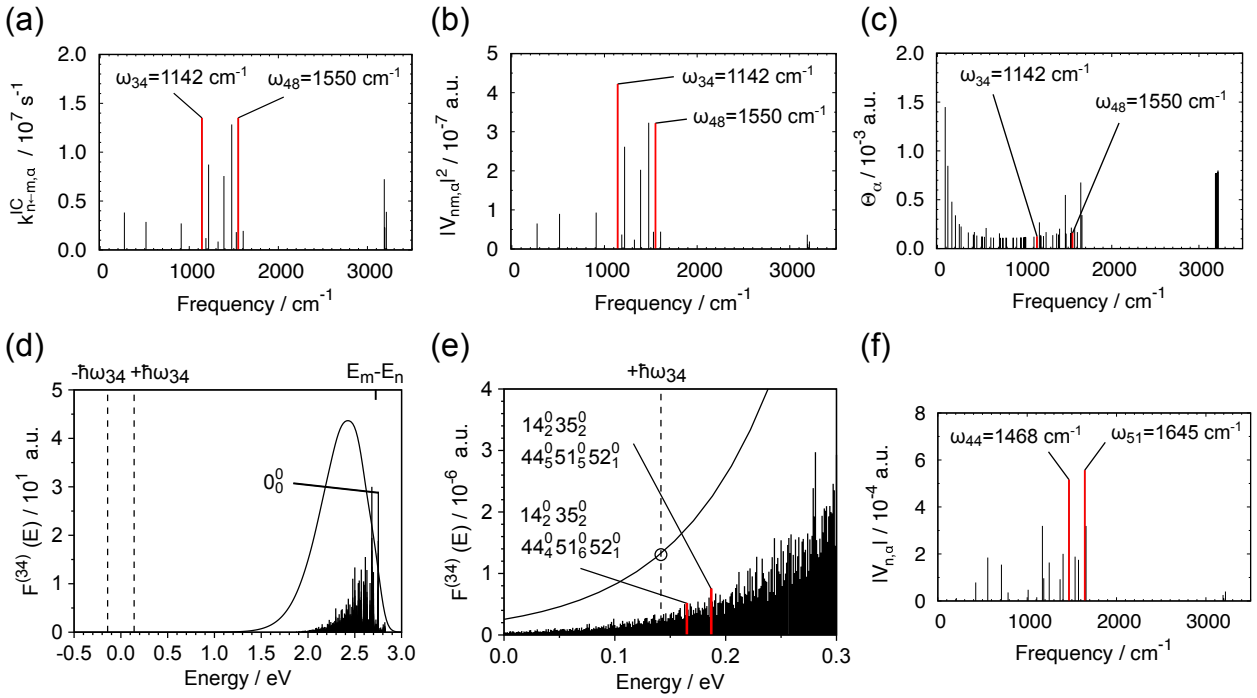

Figure 3: (a) IC rate constants, $k^{\rm IC}_{n\leftarrow m,\alpha}$, (b) square of off-diagonal VCCs, $|V_{nm,\alpha}|^2$, and (c) final density of vibronic states weighted by vibrational matrix element, Θ_α, plotted with respect to vibrational modes. $k^{\rm IC}_{n\leftarrow m,\alpha}$ and $V_{nm,\alpha}$ are non-vanishing only when $\Gamma_\alpha = B_2$. The primary promoting modes are modes 34 and 48. (d) FC envelope, $F^{(\alpha)}(E) = F^{(34)}(E)$, with promoting mode 34 dropped, and (e) its enlarged view around $E = +\hbar\omega_{34}$. The energy reference is the difference between the initial and final vibronic energies. Vertical lines show the intensities of the FC factors excluding mode 34. (f) Diagonal VCCs, $|V_{n,\alpha}|$, of S_0, which are non-vanishing when $\Gamma_\alpha = A_1$. The primary accepting modes are modes 44 and 51.

Figures 3 (d) and (e) show the FC factors (vertical lines) and FC envelope $F^{(\alpha)} = F^{(34)}$

with promoting mode 34 dropped (Eq. (21)). The FC factor of the 0–0 transition is located at $E = 2.75$ eV, corresponding to the electronic energy gap. The FC envelope decays exponentially as the energy decreases from its maximum and has a larger value at $E = +\hbar\omega_{34}$ than $E = -\hbar\omega_{34}$. This result indicates that the IC from S_1 to S_0 proceeds mainly through phonon emission rather than absorption (Table S4). Note also that spontaneous phonon emission is the dominant process because the vibrational excited states of mode 34 with a large frequency ($\omega_{34} = 1142$ cm^{-1}) are hardly populated at $T = 300$ K. The vibrational assignments of the FC factors providing the largest and second largest contributions to phonon emission were determined to be $14_2^0 35_2^0 44_5^0 51_5^0 52_1^0$ and $14_2^0 35_2^0 44_4^0 51_6^0 52_1^0$, respectively, where $\beta_{\nu'_\beta}^{\nu_\beta}$ denotes the transition from ν_β to ν'_β for mode β. These vibrational modes that constitute the final vibronic states are the accepting modes belonging to the A_1 irreducible representation. In particular, the primary accepting modes are modes 44 and 51, in which highly vibrational excited states are involved. Figure S3 shows the FC envelope with promoting mode 48 dropped, where the primary accepting modes are modes 44 and 51. These accepting modes have the largest and second-largest diagonal VCCs of S_0 (Fig. 3 (f), see Fig. S4 for the dimensionless diagonal VCCs).

Next, we discuss the dependence of the IC rate constant on the electronic energy gap, as well as the frequencies of the diagonal and off-diagonal VCCs. Figure 4 (a) shows the rate constant of 9-fluorenone plotted by changing the energy gap while fixing the other parameters. The logarithm of the rate constant increases linearly with a decreasing energy gap when the energy gap is large, as predicted by the energy gap law in the weak coupling limit.[9,10] As the energy gap decreases, the rate constant reaches a maximum and then falls. This behavior reflects the lineshape of the FC envelope. Eq. (13) indicates that the maximum value of the FC envelope depends on the electronic energy gap. As the energy gap decreases, the maximum of the FC envelope shifts to a lower energy. As indicated by the red curve in Fig. S5, the rate constant reaches a maximum value when the FC envelope becomes the largest at the energy of the emitted phonon. In the negative energy gap, or when the final

electronic state is higher than the initial state, the IC proceeds mainly through phonon absorption rather than emission (see Table S5). This process with a negative energy gap is a reverse internal conversion process.

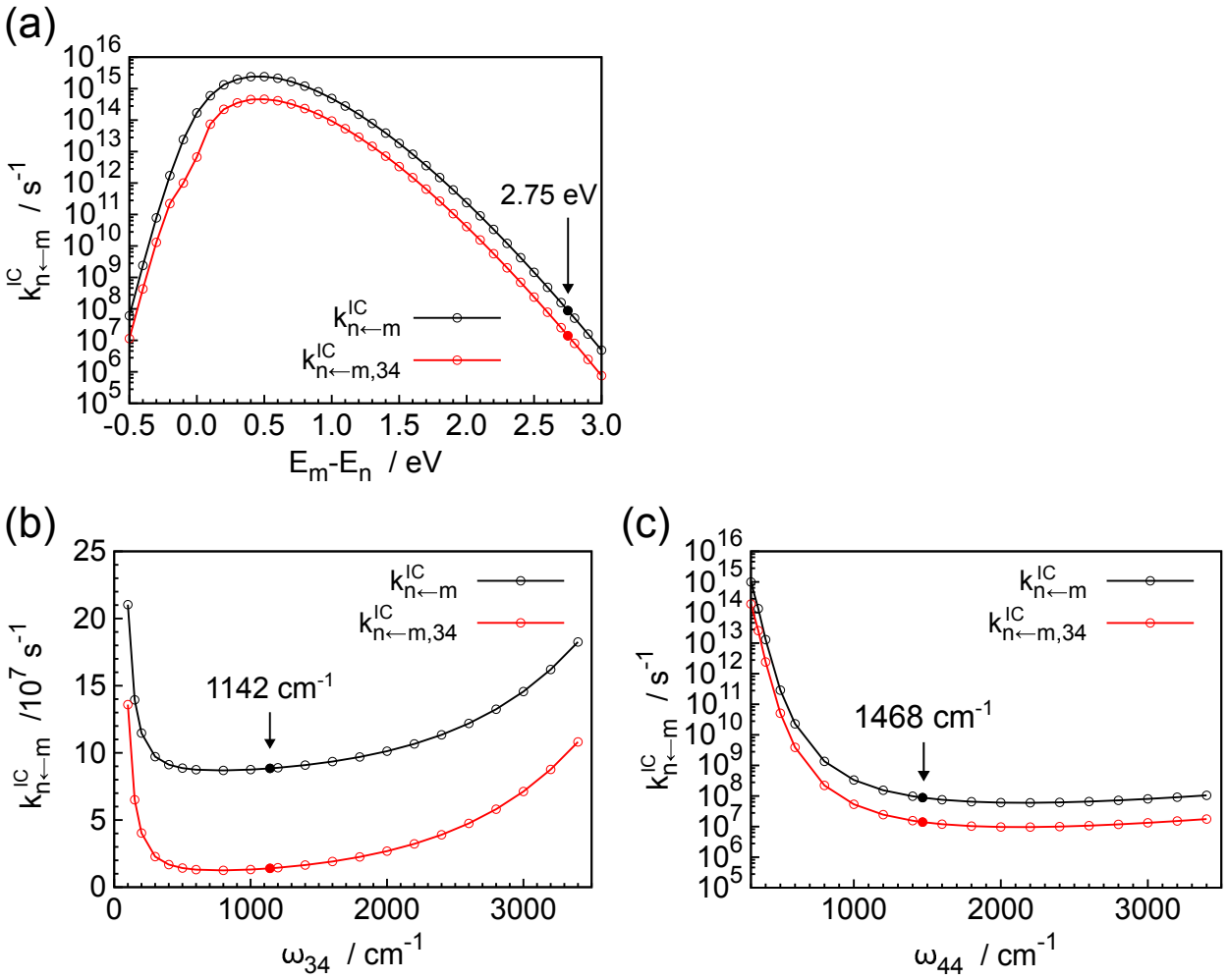

Figure 4: Dependence of the IC rate constant, $k^{\mathrm{IC}}_{n\leftarrow m}$, on the (a) electronic energy gap, $E_m - E_n$, (b) frequency of promoting mode 34, ω_{34}, and (c) frequency of accepting mode 44, ω_{44}, with the other parameters fixed. The filled circles represent the calculated rate constants of 9-fluorenone.

Figures 4 (b) and (c) show the IC rate constant plotted by changing the frequencies of primary promoting mode 34 and accepting mode 44. The rate constant is large at the low and high promoting mode frequencies compared with the middle frequencies. A low frequency increases the rate constant because the rate constant depends on the inverse of the promoting mode frequency (Eq. (12)). A high promoting mode frequency also increases

the rate constant because $F^{(\alpha)}(+\hbar\omega_\alpha)$ takes a large value when $\hbar\omega_\alpha$ is large (Eq. (12)). The balance between these two contributions determines the minimum of the rate constant with respect to the promoting mode frequency. The dependence of the rate constant on the accepting mode frequency is more significant than that on the promoting mode frequency. The rate constant drastically increases with decreasing frequency of the accepting mode. This is because the large displacement of the potential energy surface arising from the large diagonal VCC and the small frequency broadens the FC envelope (Fig. S6). These results suggest that flexible molecules are likely to exhibit faster ICs than rigid molecules.[1] Note, however, that anharmonicity is strong for such a vibrational mode with a large displacement; therefore, this effect should be considered for a more quantitative discussion.

Vibronic Coupling Density Analysis

It was found that for the IC from S_1 to S_0 in 9-fluorenone, the primary promoting modes were modes 34 and 48, giving the large off-diagonal VCCs. Meanwhile, the primary accepting modes were modes 44 and 51, giving the large diagonal VCCs. The VCDs were calculated for these modes to reveal the spatial distribution of the VCCs. Figure 5 illustrates the off-diagonal VCD analysis between S_1 and S_0 for vibrational mode 34. Since S_1 mainly consists of the HOMO-LUMO transition (Table S1), the overlap density between S_1 and S_0 can be approximately expressed as the product of the HOMO and LUMO. The overlap density has a large distribution on the C1-C2 and C9-C9a bonds, which couples strongly to the potential derivative of mode 34 with the C1-C2 and C9-C9a vibrations. Consequently, the off-diagonal VCD localizes on these bonds, where the spatial integration of such VCD does not cancel (Fig. S1). The atomic decomposition of the off-diagonal VCC of mode 34 is large at the C2, C9, and C9a sites. The overlap density also couples to the potential derivative of mode 48 distributed on the C1-C2 and C9-C9a bonds (Fig. S7), and the off-diagonal VCC of this mode originates from the same sites as those of mode 34.

Figures S8 and S9 show the diagonal VCD analyses of S_0 for vibrational modes 44 and

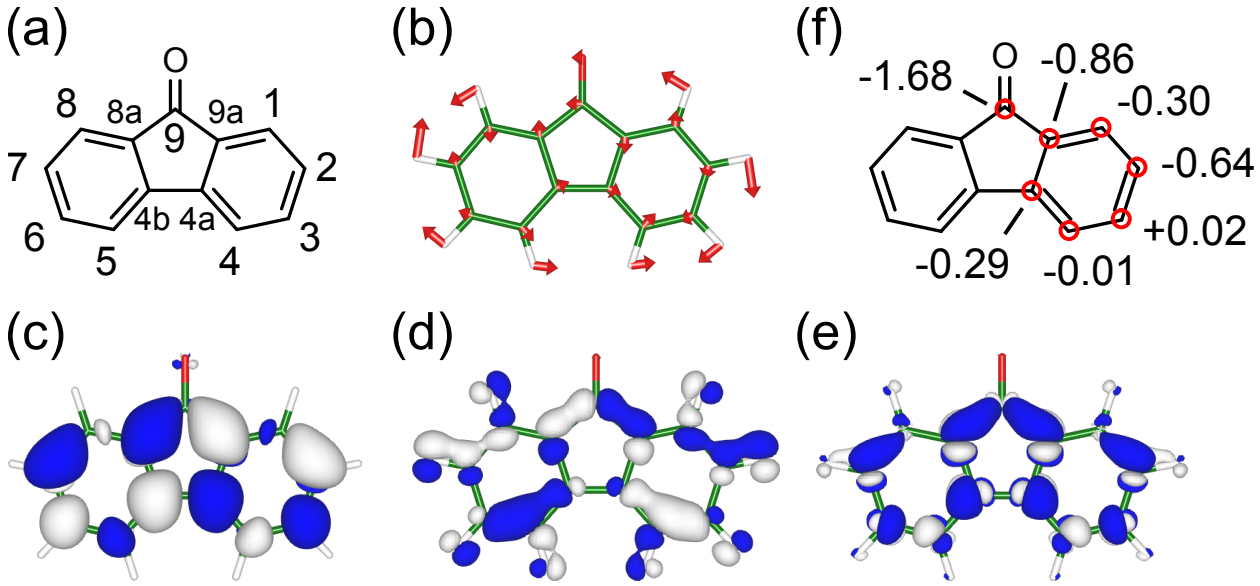

Figure 5: (a) Atomic labels of 9-fluorenone, (b) vibrational mode 34, (c) overlap density between S_1 and S_0, ρ_{nm}, (d) potential derivative of mode 34, v_α, and (e) off-diagonal VCD between S_1 and S_0 for mode 34, $\eta_{nm,\alpha}$. (f) Atomic decomposition of the off-diagonal VCC of mode 34 in 10^{-4} a.u., which is large in the C2, C9, and C9a sites. Isosurface values of ρ_{nm}, v_α, and $\eta_{nm,\alpha}$ are 1×10^{-3}, 5×10^{-3}, and 5×10^{-6} a.u., respectively. The white/blue region is positive/negative.

51, respectively. The electron density difference between S_1 and S_0 can be approximately expressed as the difference between the HOMO and LUMO densities. The electron density difference with a large distribution on the C3-C4 and C4-C4a bonds couples strongly to the potential derivatives of modes 44 and 51 with the C3-C4 and C4-C4a vibrations. Therefore, the diagonal VCCs of these modes originate mainly from the C3, C4, and C4a sites. The diagonal and off-diagonal VCCs have different origins owing to the dissimilar distributions of the electron density difference and overlap density. The introduction of substituents on the C1 and C2 to reduce the overlap density on these sites can decrease the off-diagonal VCC. Meanwhile, that on the C3 and C4 to reduce the electron density difference can decrease the diagonal VCC. As a result, both cases yield a suppressed IC rate.

The rate constant of fluorescence is proportional to the square of the transition dipole moment (Eq. (16)). The spatial distribution of the transition dipole moment is elucidated based on its density form, or transition dipole moment density (TDMD, Sec. S10).[27] Fig-

ure S10 illustrates the TDMD analysis between S_1 and S_0 in the y-direction, where the transition dipole moment is non-vanishing only in this direction, owing to the selection rule. The TDMD has a large distribution at the C2 site, indicating that the transition dipole moment originates mainly from this site.

CONCLUSION

We derived an analytical expression for the IC rate constant in a molecule based on the CA representation, where all vibrational modes were treated equally. The IC can be regarded as a phonon analog of the radiative transition; the IC proceeds through the one-phonon emission and absorption for a promoting mode, while the excess electronic energy is received by the final density of vibronic states that consists of the accepting modes. The promoting and accepting modes are defined by vibrational modes that provide non-vanishing off-diagonal and diagonal VCCs, respectively, whose irreducible representations are determined from the selection rule of vibronic couplings. The advantages of the present approach are as follows:

1. The analysis of the rate constant based on the present expression can provide novel chemical insights into IC processes.

2. The application to rational molecular design is possible by utilizing the VCD that visualizes the spatial distribution of vibronic couplings.

3. As long as the harmonic approximation is valid, the geometry optimization of the final electronic state is unnecessary because the vibronic Hamiltonian at the initial nuclear configuration contains the parameters required for a rate constant calculation.

By using 9-fluorenone as an example, we identified the key promoting and accepting modes that primarily contribute to the IC processes and revealed the origins of the vibronic couplings for these modes. The FC envelope that describes the final density of the vibronic states elucidated the rate constant dependence on the electronic energy gap and accepting modes'

frequencies, suggesting that flexible molecules with a small energy gap exhibit fast ICs. This study facilitates the quantitative and qualitative understanding of IC processes in conjunction with molecular structures; therefore, we expect that it will advance the engineering of vibronic couplings, or vibronics.[25,50]

Acknowledgement

This study was supported by JSPS KAKENHI Grant Number JP22H02157 in Scientific Research (B), and JP22K05253 in Scientific Research (C). Numerical calculations were partly performed at Supercomputer System, Institute for Chemical Research, Kyoto University, Academic Center for Computing and Media Studies (ACCMS), Kyoto University, the information initiative center, Hokkaido University, and Research Center for Computational Science, Okazaki (Project: 22-IMS-C065). We would like to thank Editage (www.editage.com) for English language editing.

Supporting Information Available

- Supporting Information: Theoretical details and supplementary computational results.

AUTHOR INFORMATION

Author Contributions

The manuscript was written through contributions of all authors.

Notes

The authors declare no competing financial interest.

References

(1) Turro, N. J.; Ramamurthy, V.; Ramamurthy, V.; Scaiano, J. C. *Principles of Molecular Photochemistry: An Introduction*; University Science Books: Sausalito, CA, 2009.

(2) Medvedev, E. S.; Osherov, V. I. *Radiationless Transitions in Polyatomic Molecules*; Springer-Verlag: New York, 1995.

(3) Nitzan, A. *Chemical Dynamics in Condensed Phases: Relaxation, Transfer and Reactions in Condensed Molecular Systems*; Oxford University Press: Oxford, 2006.

(4) Kubo, R.; Toyozawa, Y. Application of the method of generating function to radiative and non-radiative transitions of a trapped electron in a crystal. *Prog. Theor. Phys.* **1955**, *13*, 160–182.

(5) Lin, S. H. Rate of Interconversion of Electronic and Vibrational Energy. *J. Chem. Phys.* **1966**, *44*, 3759–3767.

(6) Siebrand, W. Radiationless Transitions in Polyatomic Molecules. I. Calculation of Franck—Condon Factors. *J. Chem. Phys.* **1967**, *46*, 440–447.

(7) Lin, S. H.; Bersohn, R. Effect of Partial Deuteration and Temperature on Triplet-State Lifetimes. *J. Chem. Phys.* **1968**, *48*, 2732–2736.

(8) Bixon, M.; Jortner, J. Intramolecular Radiationless Transitions. *J. Chem. Phys.* **1968**, *48*, 715–726.

(9) Englman, R.; Jortner, J. The Energy Gap Law for Radiationless Transitions in Large Molecules. *Mol. Phys.* **1970**, *18*, 145–164.

(10) Freed, K. F.; Jortner, J. Multiphonon Processes in the Nonradiative Decay of Large Molecules. *J. Chem. Phys.* **1970**, *52*, 6272–6291.

(11) Hayashi, M.; Mebel, A. M.; Liang, K. K.; Lin, S. H. Ab Initio Calculations of Radiationless Transitions between Excited and Ground Singlet Electronic States of Ethylene. *J. Chem. Phys.* **1998**, *108*, 2044–2055.

(12) Mebel, A.; Hayashi, M.; Liang, K.; Lin, S. Ab initio calculations of vibronic spectra and dynamics for small polyatomic molecules: Role of Duschinsky effect. *J. Phys. Chem. A* **1999**, *103*, 10674–10690.

(13) Niu, Y.; Peng, Q.; Shuai, Z. Promoting-Mode Free Formalism for Excited State Radiationless Decay Process with Duschinsky Rotation Effect. *Sci. China Ser. B: Chem.* **2008**, *51*, 1153–1158.

(14) Niu, Y.; Peng, Q.; Deng, C.; Gao, X.; Shuai, Z. Theory of Excited State Decays and Optical Spectra: Application to Polyatomic Molecules. *J. Phys. Chem. A* **2010**, *114*, 7817–7831.

(15) Shuai, Z. Thermal Vibration Correlation Function Formalism for Molecular Excited State Decay Rates. *Chin. J. Chem.* **2020**, *38*, 1223–1232.

(16) Etinski, M.; Tatchen, J.; Marian, C. M. Time-Dependent Approaches for the Calculation of Intersystem Crossing Rates. *J. Chem. Phys.* **2011**, *134*, 154105.

(17) Baiardi, A.; Bloino, J.; Barone, V. General Time Dependent Approach to Vibronic Spectroscopy Including Franck–Condon, Herzberg–Teller, and Duschinsky Effects. *J. Chem. Theory Comput.* **2013**, *9*, 4097–4115.

(18) Peng, Q.; Niu, Y.; Shi, Q.; Gao, X.; Shuai, Z. Correlation Function Formalism for Triplet Excited State Decay: Combined Spin–orbit and Nonadiabatic Couplings. *J. Chem. Theory Comput.* **2013**, *9*, 1132–1143.

(19) Baiardi, A.; Bloino, J.; Barone, V. A General Time-Dependent Route to Resonance-

Raman Spectroscopy Including Franck-Condon, Herzberg-Teller and Duschinsky effects. *J. Chem. Phys.* **2014**, *141*, 114108.

(20) de Souza, B.; Neese, F.; Izsák, R. On the Theoretical Prediction of Fluorescence Rates from First Principles Using the Path Integral Approach. *J. Chem. Phys.* **2018**, *148*, 034104.

(21) de Souza, B.; Farias, G.; Neese, F.; Izsák, R. Predicting Phosphorescence Rates of Light Organic Molecules Using Time-Dependent Density Functional Theory and the Path Integral Approach to Dynamics. *J. Chem. Theory Comput.* **2019**, *15*, 1896–1904.

(22) Fischer, G. *Vibronic Coupling: The Interaction between the Electronic and Nuclear Motions*; Academic Press: London, 1984.

(23) Azumi, T.; Matsuzaki, K. What Does the term "Vibronic Coupling" Mean? *Photochem. Photobiol.* **1977**, *25*, 315–326.

(24) Kato, T.; Haruta, N.; Sato, T. *Vibronic Coupling Density: Understanding Molecular Deformation*; Springer: Singapore, 2021.

(25) Sato, T.; Tokunaga, K.; Iwahara, N.; Shizu, K.; Tanaka, K. In *The Jahn-Teller Effect: Fundamentals and Implications for Physics and Chemistry*; Köppel, H., Yarkony, D. R., Barentzen, H., Eds.; Springer-Verlag: Berlin and Hidelberg, 2009; pp 99–129.

(26) Sato, T.; Tokunaga, K.; Tanaka, K. Vibronic Coupling in Naphthalene Anion: Vibronic Coupling Density Analysis for Totally Symmetric Vibrational Modes. *J. Phys. Chem. A* **2008**, *112*, 758–767.

(27) Uejima, M.; Sato, T.; Yokoyama, D.; Tanaka, K.; Park, J.-W. Quantum Yield in Blue-Emitting Anthracene Derivatives: Vibronic Coupling Density and Transition Dipole Moment Density. *Phys. Chem. Chem. Phys.* **2014**, *16*, 14244–14256.

(28) Uejima, M.; Sato, T.; Detani, M.; Wakamiya, A.; Suzuki, F.; Suzuki, H.; Fukushima, T.; Tanaka, K.; Murata, Y.; Adachi, C.; Kaji, H. A Designed Fluorescent Anthracene Derivative: Theory, Calculation, Synthesis, and Characterization. *Chem. Phys. Lett.* **2014**, *602*, 80–83.

(29) Uejima, M.; Sato, T.; Tanaka, K.; Kaji, H. Enhancement of Fluorescence in Anthracene by Chlorination: Vibronic Coupling and Transition Dipole Moment Density Analysis. *Chem. Phys.* **2014**, *430*, 47–55.

(30) Sato, T.; Hayashi, R.; Haruta, N.; Pu, Y.-J. Fluorescence via Reverse Intersystem Crossing from Higher Triplet States in a Bisanthracene Derivative. *Sci. Rep.* **2017**, *7*, 1–9.

(31) Ota, W.; Takahashi, K.; Higashiguchi, K.; Matsuda, K.; Sato, T. Origin of Aggregation-Induced Enhanced Emission: Role of Pseudo-Degenerate Dlectronic States of Excimers Formed in Aggregation Phases. *J. Mater. Chem. C* **2020**, *8*, 8036–8046.

(32) Kimura, S.; Uejima, M.; Ota, W.; Sato, T.; Kusaka, S.; Matsuda, R.; Nishihara, H.; Kusamoto, T. An Open-Shell, Luminescent, Two-Dimensional Coordination Polymer with a Honeycomb Lattice and Triangular Organic Radical. *J. Am. Chem. Soc.* **2021**, *143*, 4329–4338.

(33) Sato, T.; Ota, W.; Hira, S.; Uejima, M.; Sakanoue, K.; Fujiwara, E.; Sato, T. (Kyoto University). Light-Emitting Material, OLED and Compound. Worldwide patent WO2021117809, 2021.

(34) Sato, T.; Ota, W.; Hira, S.; Uejima, M.; Sakanoue, K.; Sato, T. (Kyoto University). Preparation of Boron-Containing Heterocyclic Compound for Organic Light-Emitting Element. Worldwide patent WO2021153168, 2021.

(35) Sato, T.; Ota, W.; Hira, S.; Uejima, M.; Sakanoue, K. (Kyoto University). Com-

pound, Light-Emitting Material, and Organic Light-Emitting Element. Worldwide patent WO2022030265, 2022.

(36) Murphy, R. S.; Moorlag, C. P.; Green, W. H.; Bohne, C. Photophysical Characterization of Fluorenone Derivatives. *J. Photoche. Photobiol. A: Chem.* **1997**, *110*, 123–129.

(37) Biczók, L.; Bérces, T. Temperature Dependence of the Rates of Photophysical Processes of Fluorenone. *J. Phys. Chem.* **1988**, *92*, 3842–3845.

(38) Biczók, L.; Bérces, T.; Márta, F. Substituent, Solvent, and Temperature Effects on Radiative and Nonradiative Processes of Singlet Excited Fluorenone Derivatives. *J. Phys. Chem.* **1993**, *97*, 8895–8899.

(39) Soliverez, C. E. An Effective Hamiltonian and Time-Independent Perturbation Theory. *J. Phys. C: Solid St. Phys.* **1969**, *2*, 2161–2174.

(40) Duschinsky, F. On the Interpretation of Electronic Spectra of Polyatomic Molecules. *Acta Physicochim. URSS* **1937**, *7*, 551.

(41) Hutchisson, E. Band Spectra Intensities for Symmetrical Diatomic Molecules. *Phys. Rev.* **1930**, *36*, 410–420.

(42) Palma, A.; Morales, J. Franck–Condon Factors and Ladder Operators. I. Harmonic Oscillator. *Int. J. Quantum Chem.* **1983**, *24*, 393–400.

(43) Bersuker, I. B.; Polinger, V. Z. *Vibronic Interactions in Molecules and Crystals*; Springer-Verlag: Berlin, 1989.

(44) Sakurai, J. J. *Advanced Quantum Mechanics*; Addison-Wesley: Reading, MA, 1967.

(45) Craig, D. P.; Thirunamachandran, T. *Molecular Quantum Electrodynamics: An Introduction to Radiation-Molecule Interactions*; Dover Publications: New York, 1998.

(46) Schatz, G. C.; Ratner, M. A. *Quantum Mechanics in Chemistry*; Dover Publications: New York, 2002.

(47) Tomasi, J.; Mennucci, B.; Cammi, R. Quantum Mechanical Continuum Solvation Models. *Chem. Rev.* **2005**, *105*, 2999–3094.

(48) Frisch, M. J. et al. Gaussian 16, Revision C. 01, Gaussian, Inc.: Wallingford, CT, 2019.

(49) Biczók, L.; Bérces, T.; Inoue, H. Effects of Molecular Structure and Hydrogen Bonding on the Radiationless Deactivation of Singlet Excited Fluorenone Derivatives. *J. Phys. Chem. A* **1999**, *103*, 3837–3842.

(50) Tokunaga, K.; Sato, T.; Tanaka, K. Calculation of vibronic coupling constant and vibronic coupling density analysis. *J. Mol. Struct.* **2007**, *838*, 116–123.